SUPPLEMENTARY INFORMATION

Quantifying Apathy in Late-Life Depression: Unraveling Neurobehavioral Links Through Daily Activity Patterns and Brain Connectivity Analysis

Roy *et al.*

1. Supplementary Methods

2. Supplementary Results

Supplementary Tables

Supplementary Figures

Supplementary References

1. Supplementary Methods

1.1 Preprocessing of MRI data

Preprocessing of anatomical images consisted in skull-stripping using an atlas-registration-based method by transforming the structural image of each patient to the atlas image, using the linear and non-linear block-matching algorithm (2,3) available in the image processing toolbox Anima (https://github.com/Inria-Visages/Anima-Public/wiki).

For the fMRI images, the following preprocessing was performed. The first four volumes from each subject were discarded to allow the signal to reach equilibrium and the participants to adapt to the scanning noise. A fieldmap was estimated based on two EPI references with opposing phase-encoding directions using ***topup***. The estimated fieldmap was applied to the fMRI images using ***fugue***. Head-motion parameters with respect to the median or mean fMRI volume (transformation matrices, and six corresponding rotation and translation parameters) were estimated before applying spatiotemporal filtering using ***mcflirt***. BOLD runs were slice-time corrected using ***slicetimer***. A bandpass filtering was applied to the BOLD signal to filter time series frequencies between 0.01 and 0.1 Hz. The median fMRI volume was co-registered to the participant's structural image, using a rigid body transformation model (6 parameters). The structural image was then transformed to the Montreal Neurological Institute (MNI) template, using the linear and non-linear block-matching algorithms (2,3). For each subject, two image transformations were computed: the transformation from the mean functional volume to the structural volume and the transformation from the individual structural volume to the MNI template. By concatenating the above transformations sequentially, we obtained a direct transformation from each initial functional volume to the MNI space. The inverse of the transformation was applied to the Human Connectome Project (HCP) multimodal parcellation(4) to register this atlas in the fMRI native space. After these steps, nuisance regression was performed with 3 kinds of regressors. Residual motion was removed with the parameters estimated by FSL's ***mcflirt***, computed by backwards differences (6 regressors). The physiological noise was reduced using regressors calculated by the CompCor method (5), implemented in nilearn (http://nilearn.github.io/). These 5 regressors correspond to the principal components from noisy regions-of-non-interest, such as white matter, cerebral spinal fluid and non-brain signals. The global signal was included as a regressor by inspection of the connectivity matrix. Individual structural and functional images were inspected to remove subjects with significant artifacts or lesions. Participants were excluded if any of the following image quality metrics were above/below the specified threshold. Exclusion criteria were specified as an AFNI's mean quality index("aqi") index > 0.025, computed by the ***3dTqual*** routine (6), a signal to noise ratio < 1, a root-mean-square head motion above 2mm for translations and 1° for rotation, as accepted in elderly population (7). With these criteria, 3 LLD subjects were excluded, two for significant artifacts and one for excessive head motion.

For diffusion images, the preprocessing pipeline consisted of these following steps, using the the Anima toolbox. Eddy current correction was performed by registering linearly then non-linearly each sub-volume of the CUSP data to the first sub-volume. Each non-linear transformation is computed only in the phase encoding direction. Then, distortion correction was designed to register two b_0 images of opposite phase encoding directions using a block-matching correction (8). The transformation was applied to all diffusion-weighted images volumes to obtain an unwrapped volume. Denoising was based on a 3-D optimized blockwise version of the non-local means filter using the redundancy of information to remove the noise (9). Skull-stripping was performed on the MPRAGE image using an atlas-registration-based method. The structural image of each patient was transformed to the MNI152 atlas image (10), using the linear and non-linear block-matching algorithms (2). Finally, a rigid transformation was computed between the structural image and the diffusion-weighted image volume of the subject, and the composition of the two transformations was finally inversely applied to the atlas mask to obtain the diffusion-weighted mask.

1.2 Preprocessing of Accelerometry

Post-filtered acceleration values were summed at each axis into epochs of 30 seconds and transformed into counts values. The vector magnitude of the count in the three axes was calculated at each second. Data were first visually inspected on the Actilife® software and kept if at least 72 hours of activity were recorded (11). Recordings of accelerometry between midnight and 5 a.m. were excluded due to the high rate of estimated missing values by the accelerometer device. One subject was excluded because of insufficient recording.

Daytime motor activity was smoothed using a generalized additive mixed model (12) with a Tweedie link function, with the *mgcv* package (13) in RStudio. The model's log-likelihood was penalized by estimating a restricted maximum likelihood smoothing parameter. We chose a cyclic cubic regression spline as basis for the fixed effect of time, constraining the activity at the beginning and end of the day to have the same value and rate of change over time. We tested 5 models by combining parameters (**Supplementary Table S1**): with or without a common smoothing function and with or without a common smoothing parameter across subjects. The best model was selected based on the Akaike criterion (14), minimal mean squared error and mean total out-of-sample deviance by leave-one out cross validation score (12).

1.3 Statistical Methods

Threshold-free Network Based Statistics

The functional connectivity measures between any pair of ROIs were estimated using a Pearson's correlation. A Fisher's r-to-z transformation was applied to normalize the coefficients. The threshold-free network-based statistics (TFNBS) (15,16) combines the network-based statistics approach (15) and the threshold-free cluster enhancement algorithm adapted for graphs. The algorithm computes the likelihood of each set of connected edges that surpass an initial statistical threshold, also referred to as components of interest (COI). Such likelihood estimation is based on the number of connected edges and how it compares to a null distribution generated by permutations of the original data. However, contrary to NBS, an adaptive threshold was implemented without having to set arbitrary a priori thresholds. The method consists of the 4 following steps (see Baggio et al., 2018): (i) The z-scores are corrected for confounders of age, gender and education using a linear regression method. The association between the principal component score and the COI is investigated by three distinct linear models, one per resting state network. (ii) A threshold is applied to the obtained F-statistics matrix at a series of steps h, with a step interval defined as a hundredth of the maximum value of the matrix. (iii) At each thresholding step, the value of each matrix suprathreshold element belonging to a connected component is replaced by the component's number of connections raised to the power E, multiplied by the component's height raised to the power H. As recommended (16), the E parameter values were set to 0.75 combined with H parameter values of 3.25. (iv) The matrices obtained at each step were subsequently summed giving the final TFNBS score for every network edge. Statistical significance was established through permutation testing over 10000 permutations. At each permutation, principal component score was shuffled across subjects, and the steps above repeated. FWE-corrected p-values were obtained by comparing each connection's TFNBS score with the null distribution of maximal sub-connectome-wise scores at each permutation. The alpha FWE-corrected p-value for statistics significance of the network was set as 0.05 / number of models.

2. Supplementary Results

2.1 Association between patterns of activity and apathy in LLD controlling for depression severity

Demographic and clinical variables of the LLD group (apathetic and non-apathetic) are reported in Table S2. This provides a broad comparison between apathetic and unapathetic patients based on the 2018 Diagnostic Criteria of Apathy. However, apathy was evaluated with two more clinical scales. Twenty-seven LLD participants met the DCA criteria of apathy against eleven non-apathetic LLD. Both groups had a majority of unipolar depression, with similar proportions between the groups and an increased

depression severity tendency in the apathetic group ($p_{uncorrected}$=0.06). Apathetic and non-apathetic groups were similar in terms of age, gender, years of education and executive functions

2.2 Association between patterns of activity and apathy in LLD controlling for depression severity

As requested after review, we performed the analyses between apathy and adding the MADRS total score as covariates. As expected, we found significant or near-significant correlations between MADRS and AES ($r_{pearson}$= 0.41, p=0.008), MADRS and AMI ($r_{pearson}$= 0.31, p=0.06), as well as MADRS and DCA ($r_{pearson}$= 0.33, p=0.038). Including MADRS as a covariate in the regression model, we found a strengthened association between AES and fPC1 (t=-2.85, p=0.0073), but a slightly decreased association between AMI and fPC2 (t=-2.38, p=0.02) in comparison with the model without MADRS. The association between DCA and apathy remain non significant after correction for multiple comparisons (t=-2.07, p=0.045). These results suggest that mean motor activity is associated with apathy independantly from depression symptoms severity, while the association between late-chronotype and social apathy is mildly affected by depression severity. Due to the intricacy of apathy symptoms in depression and the debated nature of apathy, as a type of depression or a distinct entity in dementia, we present these results as complementary to our main analyses.

2.3 Association between patterns of activity and functional brain connectivity in LLD controlling for duration of depression

As requested after review, we performed brain connectivity analyses controlling for disease duration because of the variability of disease duration within the sample.

The effect of mean diurnal activity on functional connectivity with disease duration, we found similar results our original analysis. The significant intra-DMN network had 98.6% overlapping regions than our original model (5 new regions and 6 not found anymore), 97.6% overlapping regions for the CON (11 new regions found and 11 not found anymore) and 96.8% for the FPN (10 new regions found and 14 not found anymore).

The effect of chronotype on functional connectivity with disease duration was also similar to our original analysis. The significant intra-DMN network had 98.6% overlapping regions than our original model (8 new regions and 6 not found anymore), 97.6% overlapping regions for the CON (7 new regions found and 7 not found anymore) and 96.8% for the FPN (15 new regions found and 15 not found anymore).

Because multiple mechanisms could yield to persistent depression, it is unclear which confounding variables we are accounting for and whether they should or should not be taken into consideration to

measure the relationship between brain connectivity and motor activity. We decided to report this result in complement to the main analyses.

3. Supplementary Tables

Model	Degrees of freedom	AIC	MSE	Mean out-of-sample deviance
Mod_S	487	**511 440**	**0.45**	**13 178**
Mod_I	392	562 348	0.45	13 260
Mod_GI	355	562 745	0.45	13 470
Mod_G	48	568 422	0.47	15 573
Mod_GS	1143	527 011	2.26	16 421

Table S1. Model fits comparison of predicted smoothed accelerometry data

We compared five generalized additive models of motor activity as a function of time: model G (mod_G) corresponding to a global smoother across subjects, model GS (mod_GS) which has a global smoother plus group-level smoothers that have the same wiggliness (or a shared penalty), model GI (mod_GI) which has a global smoother plus group-level smoothers with individual wiggliness (or individual penalties), model S (mod_S) with group-specific smoothers without a global smoother but with the same wiggliness, and model I (mod_I) corresponding to group-specific smoothers with different wiggliness. Model I was selected for principal component analysis as it had the lowest AIC, MSE and mean out-of-sample deviance. ***Acronyms:*** *AIC: Akaike Information Criterion; MSE: Mean-Squared Error.*

	LLD Apathetic (n = 27)	**LLD Non-apathetic (n = 11)**	**Statistics**	**p-value**	**LLD Total (n = 38)**
Age (years)	75 72 – 81	72 71 – 78	t = 1.22	$p = 0.23$	74 72 – 80.75
Gender (M:F)	11:16	1:10	$\chi^2 = 2.31$	$p = 0.13$	12:26
Education (years)	10 8 – 12.5	12 11 - 15	t = -1.61	$p = 0.13$	12 8 – 13.75
Medical comorbidities					
Cardiovascular	11%	18%	$\chi^2 = 0.26$	$p = 0.61$	13%
Neurological	0%	0%			0%
Pneumological	4%	10%	$\chi^2 = 0.40$	$p = 0.52$	16%
Rhumatological	11%	27.3%	$\chi^2 = 1.06$	$p = 0.30$	5%
Depression characteristics					
Type of depression (MDD : Bipolar disorder)	21:6	10:1	$\chi^2 = 0.01$	$p = 0.92$	31:7
Duration of depression (years)	25 7 - 40	22 1 - 48	U = 119	$p = 0.85$	24 4 – 40
MADRS	27 25 - 30	22 21 - 27	t = 1.94	$p = 0.06$	25 22 – 30
Apathy					

AES	48 40 – 52	34 32 – 39	t = 3.72	$p < 0.001$	42 37 – 50
AMI	33 29 – 36	20 18 – 24	t = 4.82	$p < 0.001$	30 18 – 36
Psychotropic drugs (1 or more per subject)					
Antidepressants	85%	82%	$\chi^2 = 0.25$	$p = 0.88$	84%
Mood Stabilizers	15%	9%	$\chi^2 = 0.47$	$p = 0.79$	13%
Benzodiazepines	37%	45%	$\chi^2 = 0.23$	$p = 0.89$	39%
Antipsychotic	15%	0%	$\chi^2 = 0.58$	$p = 0.44$	11%
Cognitive Evaluation					
DRS	132 128 – 136	136 132 – 141	t = -1.20	p = 0.24	134 128 – 137
TMT-A	54 36.5 – 67.0	39.0 35.0 – 51.5	U = 108.5	$p = 0.20$	47.5 36.0 – 64.8
Stroop interference score	-73.5 -92.3 – -54.0	-73.5 -106.0 – -60.75	U = 103.5	$p = 0.36$	-73.5 -97.3 – -54.8
TMT B-A	76.0 48.8 – 139.5	80.0 69.0 – 100.0	U = 127	$p = 0.89$	80.0 57.0 – 124.0
MCST perseverative errors	3.5 1.8 – 6.0	1.5 0.3 – 3.0	U = 79	$p = 0.12$	3.0 1.0 – 5.8

MCST Complete categories	6.0 4.0 – 6.0	6.0 4.3 – 6.0	U = 124.5	$p = 1$	6.0 4.0 – 6.0
Verbal Fluencies Semantic	22.0 18.0 – 27.0	26.0 22 – 29.9	t = -2.21	***p = 0.03***	23.5 18.0 – 28.3
Phonemic	18.0 10.8 – 23.8	21 14.5 – 24.5	t = -0.57	$p = 0.58$	18.0 13.0 – 24.0

Table S2. Demographic and clinical data in apathetic and non-apathetic LLD groups

The entire LLD group was used for further analyses. Here, we present the apathetic and non-apathetic depression groups, based on the diagnostic criteria of apathy, to describe the participants characteristics with and without significant apathy impacting functioning.

Summary descriptive results: *Mean, minimum – maximum.* ***Acronyms:*** *AES: Apathy Evaluation Scale; AMI: Apathy Motivation Index; LLD: Late-Life Depression participants, MCST: Modified Card Sorting Test; MDRS: Mattis Dementia Rating Scale; TMT-A: Trail A of the Trail Making test; TMT B-A: difference in scores between versions B and A of the Trail.*

Apathy Measures	fPC1		fPC2		fPC3		fPC4	
	t-value	p-value	t-value	p-value	t-value	p-value	t-value	p-value
AES	**-2.85**	**0.007**	-1.35	0.185	0.59	0.56	-0.73	0.47
AMI	-0.02	0.24	-2.38	0.02	-0.17	0.48	-0.68	0.50
DCA	-1.09	0.28	--2.07	0.045	-1.18	0.25	-1.00	0.33

Table S3. Associations between principal components scores and apathy controlling for depression severity

Statistically significant associations between functional principal components (fPC) and apathy measures are reported in bold. Significant p-value had to be less than 0.017 (0.05/3) to correct for the number of apathy variables tested. ***Acronyms:*** *AES: Apathy Evaluation Scale; AMI: Apathy Motivation Index; DCA: Diagnostic Criteria for apathy, fPC#, functional principal component number #.*

Region	ROI		Association with fPC1	Association with fPC2
DMN				
Frontal polar	10d	Left	-4.84	2.32
		Right	-1.93	-1.61
	10pp	Left	-3	2.53
		Right	-3.51	2.74
	10r	Left	-1.75	-1.46
		Right	-	-0.42
Superior Frontal Cortex	8Ad	Left	-3.57	-3.05
		Right	-3.71	2.25
	8Av	Left	2.35	4.8
		Right	-0.05	-2.3
	8BL	Left	-0.17	2.09
		Right	-2.08	-
	9a	Left	-1.92	-
		Right	-3.44	-
	9m	Left	-0.36	-1.69
		Right	-1.98	-
	9p	Right	-0.78	3.18
Inferior Frontal Cortex	47l	Left	-0.19	2.9
		Right	-2.61	1.98
	47s	Left	-2.39	-0.59
		Right	-2.02	-
Orbital Frontal Cortex	47m	Left	2.24	-2.96
		Right	-0.88	1.28
	OFC	Left	-2.36	0.36
		Right	-4.09	-2.34
subgenual ACC	25	Left	2.19	-1.03
		Right	-1.09	-3.6
	10v	Left	-3.72	-1.83
		Right	-2.58	3.18
	s32	Left	-2.52	1.84

		Right	-0.35	0.56
pregenual ACC	a24	Left	-2.19	-4.84
		Right	-3.97	-2.78
dorsal ACC	d32	Left	-4.18	2.09
		Right	-2.74	-2.48
	p32	Left	-0.46	-2.29
		Right	-2.78	-1.8
PCC	23d	Left	-2.13	-3.41
		Right	0.06	-1.95
	31a	Left	2.34	-2.35
		Right	-1.03	-4.52
	31pd	Left	-5.01	3.77
		Right	-2.87	-0.73
	31pv	Left	-1.13	4.3
		Right	-1.76	0.28
	d23ab	Left	1.02	3.15
		Right	-2.97	3.74
	POS1	Left	3.29	-0.64
		Right	3.17	-3.98
	v23ab	Left	0.99	-2.3
		Right	-0.69	-1.33
Precuneus	7m	Left	1.79	2.43
		Right	-1.86	1.76
Hippocampus	H	Left	-1.22	-3.67
		Right	-1.58	0.34
Parahippocampal Cortex	EC	Left	-0.81	3.44
		Right	1.88	-
	PHA1	Left	1.18	1.73
		Right	0.62	1.47
	PHA2	Left	1.25	-1.87
		Right	-0.01	2.14
	PreS	Left	-	2.15
		Right	-2.47	-3.26

Inferior Temporal Gyrus	TE2a	Left	-	6.28
		Right	-0.84	-0.04
	TE1a	Left	-1.1	2.82
		Right	-2.15	4.97
	TE1m	Left	3.58	3.93
Temporal Pole	TGd	Left	2.21	1.6
		Right	1.47	-4.34
Superior Temporal Gyrus	STSva	Left	-0.97	-1.37
		Right	-1.19	-
	STSvp	Left	-	1.17
		Right	-0.41	1.16
Inferior Parietal Lobule	PGi	Left	-0.92	2.00
		Right	-0.72	1.79
	PGs	Left	-2.56	6.36
		Right	-0.44	2.00
FPN				
Frontal polar	a10p	Left	-1.15	1.69
		Right	-3.07	-2.68
	a47r	Left	-2.61	1.1
		Right	-3.69	-3.33
	p10p	Left	-2.79	-0.31
	p47r	Left	-3.2	-0.33
		Right	-1.73	-
Superior Frontal Cortex	8BM	Left	-1.5	-
		Right	-0.88	1.58
	i6-8	Left	-0.44	1.42
		Right	0.96	-
	s6-8	Left	0.05	-
		Right	1.86	4.52
DLPFC	8C	Left		3.92
		Right	-0.93	-1.94
	a9-46v	Left	1.42	-2.75
	p9-46v	Left	1.76	1.49

		Right	-1.56	-
Inferior Frontal Cortex	IFJp	Left	-0.86	-2.1
		Right	2.27	-
	IFSa	Left	-2.1	-1.46
		Right	-1.25	-3.52
Anterior Insula	AVI	Left	-3.53	-
		Right	-2.33	1.9
Orbital Frontal Cortex	11l	Right	-1.9	4.22
	13l	Left	1.67	-1.92
		Right	-	-1.96
Retrosplenial Cortex	RSC	Left	-1.08	-
		Right	-2.06	3.12
PCC	POS2	Left	-2.07	3.38
		Right	1.39	2.15
Precuneus	7Pm	Left	-1.24	3.45
		Right		5.27
Inferior Parietal Lobule	IP1	Left		-1.79
		Right		-3.24
	IP2	Left	-1.09	-2.95
		Right	0.21	3.4
	PFm	Left	-3.12	-1.97
		Right	-0.31	-5.2
Middle Temporal Gyrus	TE1p	Left	-1.53	-
		Right	-1.79	-1.55
CON				
Frontal polar	9-46d	Left	-	-1.4
		Right	-	1.92
Superior Frontal Cortex	46	Left	-2.43	-1.78
		Right	-2.32	4.13
Premotor Cortex	6r	Left	-1.45	1.69
		Right	-1.01	2.73
Paracentral Lobule	5mv	Left	-2.02	-0.03
		Right	-1.62	-0.37

	FEF	Left	2.61	-3.72
		Right	-1	2.01
Supplementary Motor Area	6ma	Left	-0.48	2.26
	SCEF	Left	2.02	-2.17
		Right	2.98	1.65
dorsal ACC	33pr	Left	2.84	4.13
		Right	-1.56	-
	a32pr	Right	-	3.26
	p24	Left	-	3.56
		Right	2.56	4.52
	p24pr	Left	-3.53	-1.28
		Right	-1.75	4.23
	p32pr	Left	-1.47	2.39
		Right	-2.3	3.33
Mid-cingulate cortex	a24pr	Left	-3.46	4.75
		Right	-1.93	2.73
PCC	23c	Left	-2.43	-2.45
		Right	-2.08	-
Anterior Insula	43	Left	-1.62	-0.91
		Right	0.69	-0.1
	FOP1	Left	-1.35	2.49
		Right	-	-2.62
	FOP3	Left	-0.77	2.41
		Right	-	-2.98
	FOP4	Left	0.11	1.97
		Right	-	-3.61
	FOP5	Left	3.51	0.55
		Right	2.04	-0.04
Middle Insula	MI	Left	-0.42	2.19
		Right	-0.3	-0.57
Posterior Insula	PI	Left	0.25	-4.22
		Right	-2.42	-2.72
	PoI1	Left	-1.48	0.02

		Right	-3.42	-
	PoI2	Left	-1.65	-1.09
		Right	-2.56	0.67
Inferior Parietal Lobule	PFop	Left	1.78	-3.91
		Right	-0.76	-1.69
Supramarginal Gyrus	PF	Left	-1.74	-
		Right	-	-2.09
	PFcm	Left	-0.42	-1.37
		Right	-	-4.27
Superior Parietal Lobule	7Am	Left	3.23	-

Table S4. Associations between principal components scores and functional brain connectivity

Brain ROIs significantly associated with functional principal components (fPC) of motor activity via TFNBS. The direction of the association is given by estimated marginal effect at the ROI level of the interaction effect between ROIs correlation and fPC. For more clarity, we classify the HCP's ROI label into broader brain areas following current nomenclature from the Glasser atlas (32).

Acronyms: *CON: Cingulo-Opercular Network, DMN: Default-Mode Network, fPC#, functional principal component number #, FPN: Fronto-Parietal Network.*

Tracts	DTI				NODDI			
	Fractional Anistropy		Mean Diffusivity		Orientation Dispersion Index		Partial Volume	
	Corr. Coef.	Nb of clusters > Cluster uncorrected	Corr. Coef.	Nb of clusters > Cluster uncorrected	Corr. Coef.	Nb of clusters > Cluster uncorrected	Corr. Coef.	Nb of clusters > Cluster uncorrected
CA	0.51	**2***	0.61	**1***	0.47	0	0.54	0
CC_1	-0.34	0	0.38	0	-0.32	0	-0.25	0
CC_2	-0.45	0	0.42	0	-0.49	0	0.45	0
CC_3	-0.33	0	-0.18	0	-0.41	0	-0.38	0
CC_4	-0.36	0	0.15	0	-0.35	0	0.35	0
CC_5	-0.28	0	0.50	0	-0.30	0	0.49	0
CC_6	-0.34	0	0.30	0	-0.53	**1***	0.36	0
CC_7	-0.27	0	-0.38	0	-0.37	0	0.39	0
CG_left	-0.44	**1***	0.59	**2***	-0.34	0	0.31	0
CG_right	-0.37	0	0.43	**1***	-0.36	0	0.24	0
CST_left	-0.34	0	0.47	0	-0.37	0	0.43	0
CST_right	-0.33	0	0.32	0	0.29	0	0.41	0
ILF_left	-0.31	0	0.29	0	-0.34	0	0.30	0
ILF_fight	-0.35	0	0.44	0	-0.45	0	0.38	0
SLF_I_left	-0.29	0	0.49	**1***	-0.35	0	0.35	0
SLF_I_right	-0.32	0	0.31	0	-0.40	0	0.35	0
SLF_II_left	-0.30	0	0.39	0	0.32	0	0.42	0
SLF_II_right	-0.40	0	0.39	0	-0.31	0	0.27	0
SLF_III_left	-0.52	0	0.39	0	0.36	0	0.39	0
SLF_III_right	-0.45	0	0.36	0	-0.30	0	0.30	0
UF_left	-0.38	0	0.22	0	-0.41	0	-0.33	0
UF_right	-0.34	0	0.31	0	-0.39	0	0.32	0

Table S5. **Associations between diffusion MRI metrics and first principal component of motor activity without adjustment on the number of tracts**

Along each white matter tract, significant clusters of metrics associated with fPC1 had to be greater than the familywise error rate cluster size, for a p-value of 0.05. We reported the number of significant clusters with an asterix (*) without the adjustment for multiple comparisons for the number of tracts. An adjustment is still performed for the 100 points along each tract. ***Acronyms****: DTI: Diffusion Tensor Imaging, Corr. Coef: Pearson correlation coefficient, NODDI: Neurite Orientation Dispersion and Density Imaging, fPC1: first principal component scores of motor activity.*

3. Supplementary Figures

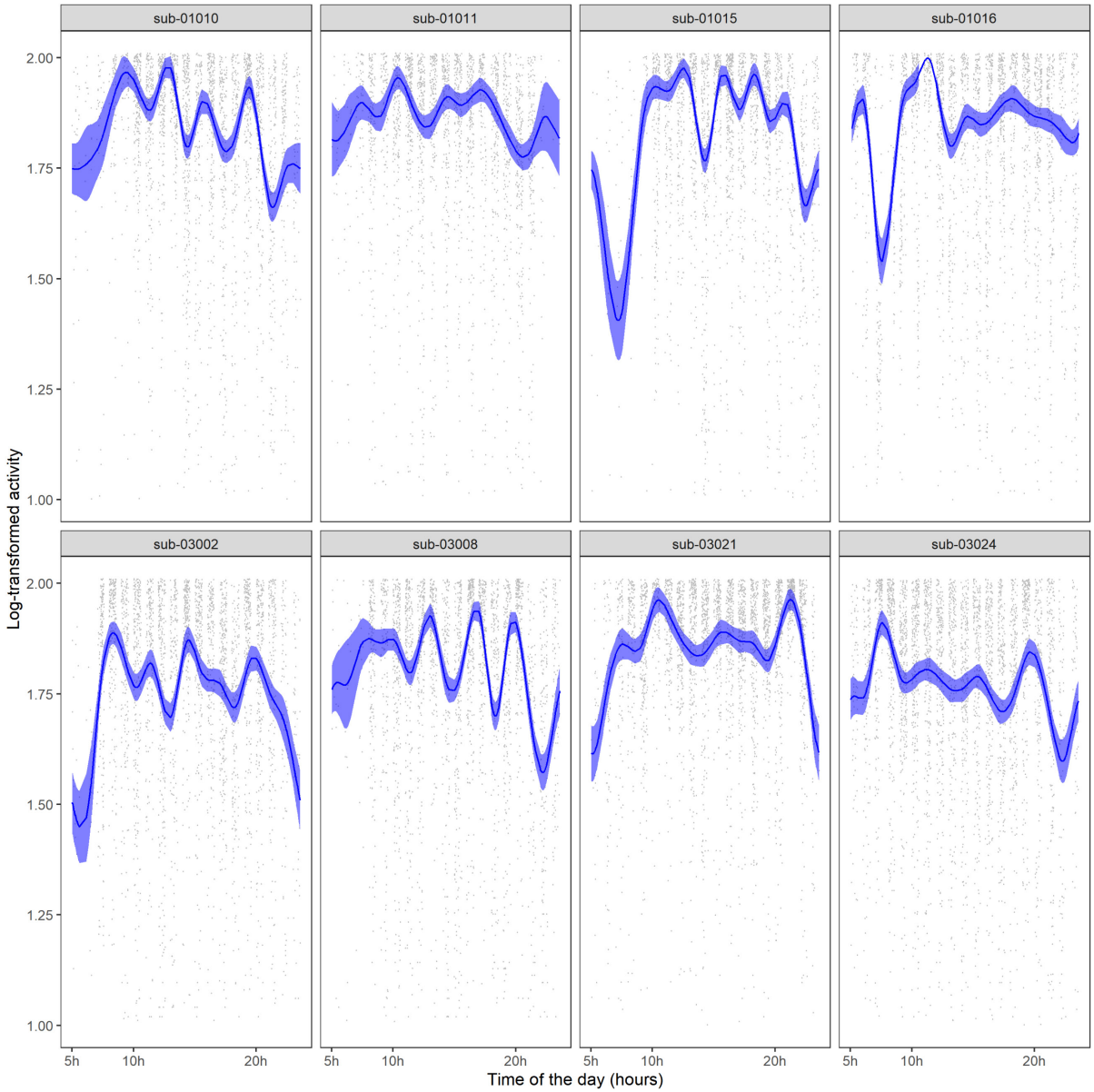

Figure S1. Examples of predicted smoothed accelerometry data from the selected model

Mean ± 2 standard errors of the predicted smooth activity as a function of time from model S are reported, against observed activity in eight randomly selected patient (4 from Rennes and 4 from Tours).

Supplementary References

1. Scherrer B, Warfield SK. Parametric Representation of Multiple White Matter Fascicles from Cube and Sphere Diffusion MRI. PLoS One. 2012 Nov 26;7(11):e48232.

2. Commowick O, Wiest-Daesslé N, Prima S. Block-matching strategies for rigid registration of multimodal medical images. In: 2012 9th IEEE International Symposium on Biomedical Imaging (ISBI). 2012. p. 700–3.

3. Ourselin S, Roche A, Prima S, Ayache N. Block Matching: A General Framework to Improve Robustness of Rigid Registration of Medical Images. In: Delp SL, DiGoia AM, Jaramaz B, editors. Medical Image Computing and Computer-Assisted Intervention – MICCAI 2000. Berlin, Heidelberg: Springer; 2000. p. 557–66. (Lecture Notes in Computer Science).

4. Glasser MF, Coalson TS, Robinson EC, Hacker CD, Harwell J, Yacoub E, et al. A multi-modal parcellation of human cerebral cortex. Nature. 2016 Aug 11;536(7615):171–8.

5. Behzadi Y, Restom K, Liau J, Liu TT. A component based noise correction method (CompCor) for BOLD and perfusion based fMRI. Neuroimage. 2007 Aug 1;37(1):90–101.

6. Cox RW. AFNI: software for analysis and visualization of functional magnetic resonance neuroimages. Comput Biomed Res. 1996 Jun;29(3):162–73.

7. Doucet GE, Labache L, Thompson PM, Joliot M, Frangou S, Alzheimer's Disease Neuroimaging Initiative. Atlas55+: Brain Functional Atlas of Resting-State Networks for Late Adulthood. Cerebral Cortex. 2021 Mar 1;31(3):1719–31.

8. Hedouin R, Commowick O, Bannier E, Scherrer B, Taquet M, Warfield SK, et al. Block-Matching Distortion Correction of Echo-Planar Images With Opposite Phase Encoding Directions. IEEE Trans Med Imaging. 2017 May;36(5):1106–15.

9. Wiest-Daesslé N, Prima S, Coupé P, Morrissey SP, Barillot C. Rician noise removal by non-Local Means filtering for low signal-to-noise ratio MRI: applications to DT-MRI. Med Image Comput Comput Assist Interv. 2008;11(Pt 2):171–9.

10. Mazziotta J, Toga A, Evans A, Fox P, Lancaster J, Zilles K, et al. A probabilistic atlas and reference system for the human brain: International Consortium for Brain Mapping (ICBM). Philos Trans R Soc Lond B Biol Sci. 2001 Aug 29;356(1412):1293–322.

11. Littner M, Kushida CA, Anderson WM, Bailey D, Berry RB, Davila DG, et al. Practice Parameters for the Role of Actigraphy in the Study of Sleep and Circadian Rhythms: An Update for 2002. Sleep. 2003 May 1;26(3):337–41.

12. Pedersen EJ, Miller DL, Simpson GL, Ross N. Hierarchical generalized additive models in ecology: an introduction with mgcv. PeerJ. 2019 May 27;7:e6876.

13. Wood SN. mgcv: GAMs and Generalized Ridge Regression for R. 2001;1.

14. Wood SN, Pya N, Säfken B. Smoothing Parameter and Model Selection for General Smooth Models. Journal of the American Statistical Association. 2016 Oct 1;111(516):1548–63.

15. Zalesky A, Fornito A, Bullmore ET. Network-based statistic: identifying differences in brain networks. Neuroimage. 2010 Dec;53(4):1197–207.

16. Baggio HC, Abos A, Segura B, Campabadal A, Garcia-Diaz A, Uribe C, et al. Statistical inference in brain graphs using threshold-free network-based statistics. Hum Brain Mapp. 2018 Jun;39(6):2289–302.